

## Extending Visual Servoing Techniques to Nonholonomic Mobile Robots

Dimitris P. Tsakiris, Patrick Rives and Claude Samson  
INRIA Sophia-Antipolis  
2004, Route des Lucioles, B.P. 93  
06902, Sophia Antipolis Cedex - France  
{first\_name}.{last\_name}@sophia.inria.fr

### Abstract

*The stabilization to a desired pose of a nonholonomic mobile robot, based on visual data from a hand-eye system mounted on it, is considered. Instances of this problem occur in practice during docking or parallel parking maneuvers of such vehicles. In this paper, we investigate the use of visual servoing techniques for their control. After briefly presenting the relevant visual servoing framework, we point out some problems encountered when it is considered for nonholonomic mobile robots. In particular, simple velocity control schemes using visual data as feedback cannot be applied anymore. We show how, by using the extra degrees of freedom provided by the hand-eye system, we can design controllers capable of accomplishing the desired task. A first approach, allows to perform a visual servoing task defined in the camera frame without explicitly controlling the pose of the nonholonomic mobile basis. A second approach based on continuous time-varying state feedback techniques allows to stabilize both the pose of the nonholonomic vehicle and that of the camera.*

*The experimental evaluation of the proposed techniques uses a mobile manipulator prototype developed in our laboratory and dedicated multiprocessor real-time image processing and control systems.*

## 1 Introduction

In order to perform a task with a mobile robot, one needs to efficiently solve many interesting problems from task planning to control law synthesis. At the control level, important results have been established for nonholonomic systems, like wheeled mobile robots, which lead to specific control problems: not only the linearization of these systems is uncontrollable, so that linear analysis and design methods cannot be applied, but also there do not exist continuous feedback control laws, involving only the state, capable of stabilizing such a system to an equilibrium, due to a topological obstruction pointed out by Brockett [1]. One of the approaches developed to solve the stabilization problem is the

use of time-varying state feedback, i.e. control laws that depend explicitly, not only on the state, but also on time, usually in a periodic way, which Samson [13] introduced in the context of the unicycle's point stabilization. This sparked a significant research effort (see for example [2] for a comprehensive survey), which demonstrated the existence of efficient such feedback control laws and provided some design procedures.

These results can be very useful in sensor-based control of mobile robotic systems. One of the prominent methods in this area is visual servoing, which was originally developed for manipulator arms with vision sensors mounted at their end-effector [4], [3], [5], [6]. In this paper, we point out the difficulties of transferring directly these techniques to nonholonomic mobile robots. We show, however, that by properly adding degrees-of-freedom to the nonholonomic platform, in the form of a hand-eye system, and by taking advantage of the time-varying stabilizing control schemes, it is still possible to extend visual servoing techniques to nonholonomic systems [9], [14]. For simplicity, we only consider here the planar case, where a mobile robot of the unicycle type carries an  $n$ -d.o.f. planar manipulator arm with a camera that moves parallel to the plane supporting the mobile robot. In a similar way, we only consider the kinematics model of the mobile robot which is sufficient to handle the problems due to the nonholonomic constraints.

In section 2, we model the kinematics and vision system of a nonholonomic mobile manipulator with an  $n$ -degree-of-freedom planar arm. Section 3 is dedicated to the analysis and synthesis of various visual servoing control schemes for our system. Some related experimental results are also presented.

## 2 Modeling

### 2.1 Mobile Manipulator Kinematics

We consider a mobile robot of the unicycle type carrying an  $n$ -d.o.f. planar manipulator arm with a camera mounted on its end effector (figure 1 shows the case of  $n = 3$ ).

Consider an inertial coordinate system  $\{F_O\}$  centered at a point  $O$  of the plane, a moving coordinate system  $\{F_M\}$  attached to the middle  $M$  of the robot's wheel axis and another moving one  $\{F_C\}$  attached to the optical center  $C$  of the camera. Let  $(x, y)$  be the position of the point  $M$  and  $\theta$  be the orientation of the mobile robot with respect to the coordinate system  $\{F_O\}$ ; let  $l_m$  be the distance of the point  $M$  from the first joint  $B_1$  of the  $n$ -d.o.f. planar arm, with  $l_1, \dots, l_n$  being the lengths of the links of the arm and  $\psi_1, \dots, \psi_n$  being its joint coordinates.

Let  $(x_{MC}, y_{MC}, \theta_{MC})$  represent the configuration of  $\{F_C\}$  with respect to  $\{F_M\}$ ,  $(x_{CT}, y_{CT}, \theta_{CT})$  represent the configuration of  $\{F_T\}$  with respect to  $\{F_C\}$ ,  $(x_C, y_C, \theta_C)$  represent the configuration of  $\{F_C\}$  with respect to  $\{F_O\}$  and  $(x_T, y_T, \theta_T)$  represent the configuration of  $\{F_T\}$  with respect to  $\{F_O\}$ , where  $x_T = d$  is the distance of point  $T$  from point  $O$  and  $y_T = \theta_T = 0$ .

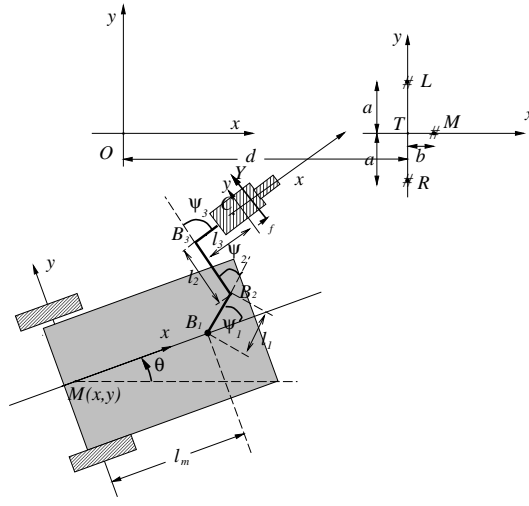


Figure 1: Mobile Manipulator with Camera

From the kinematic chain of figure 1 we have for the case of an  $n$ -degree-of-freedom manipulator arm:

$$\theta_{MC} = \sum_{i=1}^n \psi_i, \quad x_{MC} = l_m + \sum_{i=1}^n l_i \cos \left( \sum_{j=1}^i \psi_j \right), \quad y_{MC} = \sum_{i=1}^n l_i \sin \left( \sum_{j=1}^i \psi_j \right). \quad (1)$$

$$\text{and} \quad \theta_C = \theta + \sum_{i=1}^n \psi_i, \quad x_C = x + l_m \cos \theta + \sum_{i=1}^n l_i \cos \left( \theta + \sum_{j=1}^i \psi_j \right), \\ y_C = y + l_m \sin \theta + \sum_{i=1}^n l_i \sin \left( \theta + \sum_{j=1}^i \psi_j \right). \quad (2)$$

$$\text{Also} \quad \theta_{CT} = \theta_T - \theta_C, \quad x_{CT} = -(x_C - x_T) \cos \theta_C - (y_C - y_T) \sin \theta_C, \\ y_{CT} = (x_C - x_T) \sin \theta_C - (y_C - y_T) \cos \theta_C. \quad (3)$$

and

$$\theta = \theta_T - \theta_{MC} - \theta_{CT}, \\ x = x_T - x_{CT} \cos(\theta_T - \theta_{CT}) + y_{CT} \sin(\theta_T - \theta_{CT}) - x_{MC} \cos \theta + y_{MC} \sin \theta, \\ y = y_T - x_{CT} \sin(\theta_T - \theta_{CT}) - y_{CT} \cos(\theta_T - \theta_{CT}) - x_{MC} \sin \theta - y_{MC} \cos \theta. \quad (4)$$

Equations 1 and 3 are useful in simulating our system, while 2 and 4 are useful in reconstructing its state.

**Velocity Kinematics:** By differentiating the chain kinematics of the mobile manipulator and its environment, assuming that we consider stationary targets and solving for the spatial velocity of the target frame with respect to the camera frame  $\Xi^{CT}$ , we get

$$\Xi^{CT} \stackrel{\text{def}}{=} \begin{pmatrix} \dot{x}_{CT} + \dot{\theta}_{CT} y_{CT} \\ \dot{y}_{CT} - \dot{\theta}_{CT} x_{CT} \\ \dot{\theta}_{CT} \end{pmatrix} = \begin{pmatrix} B_{1,1} & B_{1,2} \end{pmatrix} \begin{pmatrix} \dot{\mathcal{X}} \\ \dot{q} \end{pmatrix}, \quad (5)$$

where  $\mathcal{X} \stackrel{\text{def}}{=} (x, y, \theta)^\top$  is the state of the mobile robot, while  $q \stackrel{\text{def}}{=} (\psi_1, \psi_2, \dots, \psi_n)^\top$  is the configuration of the manipulator arm and where the matrix  $B_{1,1}$  is

$$\begin{pmatrix} -\cos \theta_C & -\sin \theta_C & b_1^{1,1} \\ \sin \theta_C & -\cos \theta_C & b_2^{1,1} \\ 0 & 0 & -1 \end{pmatrix}, \quad (6)$$

with  $\theta_C$  given by equation 2,  $b_1^{1,1} \stackrel{\text{def}}{=} -l_m \sin(\sum_{i=1}^n \psi_i) - \sum_{i=1}^{n-1} l_i \sin(\sum_{j=i+1}^n \psi_j)$ ,  $b_2^{1,1} \stackrel{\text{def}}{=} -l_m \cos(\sum_{i=1}^n \psi_i) - \sum_{i=1}^{n-1} l_i \cos(\sum_{j=i+1}^n \psi_j) - l_n$  and the  $3 \times n$  matrix  $B_{1,2}$ , which is the Jacobian of the manipulator arm, given by

$$\begin{pmatrix} -\sum_{i=1}^{n-1} l_i \sin(\sum_{j=i+1}^n \psi_j) & \cdots & 0 \\ -\left[\sum_{i=1}^{n-1} l_i \cos(\sum_{j=i+1}^n \psi_j) + l_n\right] & \cdots & -l_n \\ -1 & \cdots & -1 \end{pmatrix}. \quad (7)$$

**Nonholonomic Constraints:** The nonholonomic constraints on the motion of the mobile robot arise from the rolling-without-slipping of the mobile platform's wheels on the plane supporting the system. Due to these constraints, the instantaneous velocity lateral to the heading direction of the mobile platform has to be zero.

From this we get the usual unicycle kinematic model for the mobile robot:

$$\dot{x} = v \cos \theta, \quad \dot{y} = v \sin \theta, \quad \dot{\theta} = \omega, \quad (8)$$

where  $v \stackrel{\text{def}}{=} \dot{x} \cos \theta + \dot{y} \sin \theta$  is the heading speed and  $\omega$  is the angular velocity of the unicycle. Then

$$\dot{\mathcal{X}} = B_{3,1}(X) \begin{pmatrix} v \\ \omega \end{pmatrix} = \begin{pmatrix} \cos \theta & 0 \\ \sin \theta & 0 \\ 0 & 1 \end{pmatrix} \begin{pmatrix} v \\ \omega \end{pmatrix}. \quad (9)$$

## 2.2 Vision Model

We consider a special case of the general visual servoing framework developed in [4], [3] and surveyed in [5], [6], [12], as it applies to a hand-eye system composed of a manipulator arm with a camera mounted on its end-effector.

Consider a fixed target containing three easily identifiable feature points arranged in the configuration of figure 1. The coordinates of the three feature points with respect to  $\{F_T\}$  are  $(x_p^{\{T\}}, y_p^{\{T\}})$ ,  $p \in \{l, m, r\}$ . The distances  $a$  and  $b$  (fig. 1) are assumed to be known. The coordinates of the feature points with respect to the camera coordinate frame  $\{F_C\}$  can be easily found.

We assume the usual pinhole camera model for our vision sensor, with perspective projection of the target's feature points (viewed as points on the plane  $\mathbb{R}^2$ ) on a 1-dimensional image plane (analogous to a linear CCD array). This defines the projection function  $\mathcal{P}$  of a point of  $\mathbb{R}^2$ , which has coordinates  $(x, y)$  with respect to the camera coordinate frame  $\{F_C\}$ , as

$$\mathcal{P} : \mathbb{R}_+ \times \mathbb{R} \longrightarrow \mathbb{R} : (x, y) \longmapsto \mathcal{P}(x, y) = f \frac{y}{x}. \quad (10)$$

where  $f$  is the focal length of the camera. In our setup, the coordinate  $x$  corresponds to "depth".

Let the projections of the target feature points on the image plane be  $Y_p = \mathcal{P}(x_p^{\{C\}}, y_p^{\{C\}})$ ,  $p \in \{l, m, r\}$ , given by 10. The vision data are then  $Y_v \stackrel{\text{def}}{=} (Y_l, Y_m, Y_r)^\top$ . Differentiating 10, we get the well-known equations of the optical flow [7] for the 1-dimensional case:

$$\dot{Y}_v = B_{2,1}(Y_p, x_p^{\{C\}}) \Xi^{CT} = \begin{pmatrix} -\frac{1}{x_l^{\{C\}}} Y_l & \frac{1}{x_l^{\{C\}}} f & \frac{1}{f}(f^2 + Y_l^2) \\ -\frac{1}{x_m^{\{C\}}} Y_m & \frac{1}{x_m^{\{C\}}} f & \frac{1}{f}(f^2 + Y_m^2) \\ -\frac{1}{x_r^{\{C\}}} Y_r & \frac{1}{x_r^{\{C\}}} f & \frac{1}{f}(f^2 + Y_r^2) \end{pmatrix} \Xi^{CT}, \quad (11)$$

where the matrix  $B_{2,1}(Y_p, x_p^{\{C\}})$  corresponds to the Jacobian of the visual data, so-called *interaction matrix* [4], [10].

### 2.3 Visual Servoing Scheme

The above modeling equations of the mobile robot with the  $n$ -d.o.f. manipulator arm can be regrouped to derive a few basic relations.

The state of the system is  $X = (\mathcal{X}, q)^\top$ . Then

$$\begin{pmatrix} \Xi^{CT} \\ \dot{q} \end{pmatrix} = B_1(X) \dot{X} = \begin{pmatrix} B_{1,1} & B_{1,2} \\ \mathbf{0}_{n \times 3} & \mathbb{I}_{n \times n} \end{pmatrix} \begin{pmatrix} \dot{\mathcal{X}} \\ \dot{q} \end{pmatrix}. \quad (12)$$

The sensory data are  $Y = (Y_v, q)^\top$ . Then

$$\dot{Y} = B_2(X) \begin{pmatrix} \Xi^{CT} \\ \dot{q} \end{pmatrix} = \begin{pmatrix} B_{2,1} & \mathbf{0}_{3 \times n} \\ \mathbf{0}_{n \times 3} & \mathbb{I}_{n \times n} \end{pmatrix} \begin{pmatrix} \Xi^{CT} \\ \dot{q} \end{pmatrix}. \quad (13)$$

The relationship between the state and the sensory data  $Y = \Phi(X)$  is given by equations 10, 11, 5 and 12. The corresponding differential relationship is

$$\dot{Y} = \frac{\partial \Phi}{\partial X}(X) \dot{X} = B_2(X) B_1(X) \dot{X}. \quad (14)$$

The controls of the system are  $\mathcal{U} = (v, \omega, \omega_{\psi_1}, \dots, \omega_{\psi_n})^\top = (v, \dot{\theta}, \dot{q})^\top$ . Then

$$\dot{X} = \begin{pmatrix} \dot{x} \\ \dot{q} \end{pmatrix} = B_3(X) \mathcal{U} = \begin{pmatrix} B_{3,1} & \mathbf{0}_{3 \times n} \\ \mathbf{0}_{n \times 2} & \mathbb{I}_{n \times n} \end{pmatrix} \begin{pmatrix} v \\ \dot{\theta} \\ \dot{q} \end{pmatrix}. \quad (15)$$

### 3 Vision-based Control of Mobile Manipulators

#### 3.1 Camera Pose Stabilization:

In this first approach, we show that it is possible to use a velocity control scheme as done in the holonomic case, provided that the control objective does not require to explicitly stabilize the pose of the mobile platform.

To illustrate this possibility, we consider a reduced system with only one actuated pan-axis ( $n = 1$ ). Our objective is to stabilize the camera to a desired pose, obtained by specifying the corresponding vision data  $Y_v^* \stackrel{\text{def}}{=} (Y_l^*, Y_m^*, Y_r^*)^\top$ . We select the task output  $e(X) = Y_v - Y_v^*$ , with  $\dim e = 3$ , which we want to drive exponentially to zero.

The system state is  $X = (x, y, \theta, \psi_1)^\top$ , the measurement data are  $Y = (Y_l, Y_m, Y_r, \psi_1)^\top$  and the control is  $\mathcal{U} = (v, \omega, \omega_{\psi_1})^\top$ . From 11 we get

$$\dot{e} = \dot{Y}_v = B_{2,1}(X) \Xi^{CT} = -\lambda e. \quad (16)$$

Then, away from singularities of  $B_{2,1}$ , we have

$$\Xi^{CT} = -\lambda B_{2,1}^{-1}(X)(Y_v - Y_v^*). \quad (17)$$

From the system kinematics we have

$$\Xi^{CT} = (B_{1,1}(X) \ B_{1,2}(X)) B_3(X) \mathcal{U} = \begin{pmatrix} -\cos \psi_1 & -l_m \sin \psi_1 & 0 \\ \sin \psi_1 & -[l_m \cos \psi_1 + l_1] & -l_1 \\ 0 & -1 & -1 \end{pmatrix} \begin{pmatrix} v \\ \omega \\ \omega_{\psi} \end{pmatrix}, \quad (18)$$

where the  $3 \times 4$  matrix  $(B_{1,1} \ B_{1,2})$  is given by 6 and 7, and the  $4 \times 3$  matrix  $B_3$  is given by 15, by setting  $n = 1$ . The product  $(B_{1,1} \ B_{1,2}) B_3$  depends only on  $\psi_1$ . It is a nonsingular matrix, since its determinant is  $-l_m$ . Then

$$\mathcal{U} = \left[ (B_{1,1}(X) \ B_{1,2}(X)) B_3(X) \right]^{-1} \Xi^{CT} \quad (19)$$

and, using 17, we finally get

$$\mathcal{U} = -\lambda \left[ (B_{1,1}(X) \ B_{1,2}(X)) B_3(X) \right]^{-1} B_{2,1}^{-1}(X^*)(Y_v - Y_v^*). \quad (20)$$

Subjected to this control law, the mobile manipulator moves so that the camera asymptotically reaches its desired pose with respect to the target. However, the pose of the mobile platform itself is not stabilized, and problems of drift due

to the non-stable zero-dynamics of the system can occur. In practice, however, friction will have a stabilizing effect and the platform come to a rest. However, the final pose reached by it will still largely depend upon its initial position and orientation.

Related experimental results obtained in [9] are shown in fig. 2, where the trajectories of the system for two different initial configurations, but with the same desired camera pose with respect to the target, are plotted. The different final poses of the mobile platform can be seen.

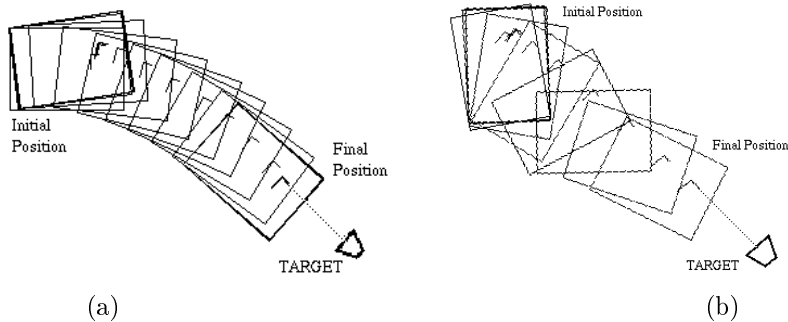


Figure 2: Robot trajectories for two different initial configurations and the same desired camera pose

### 3.2 Mobile Base Pose Stabilization:

Consider the same system as in section 3.1 (i.e. the mobile robot with only one actuated pan-axis). Its state, sensory data and control input variables are also as before.

In this second approach, we consider the stabilization of the mobile platform to a desired pose with respect to some target. At the same time, we require that the camera tracks the targets, whatever the motion of the platform. The role of the arm is, in this case, to provide an extra d.o.f., which will allow the camera to move independently.

One of the approaches developed to solve the point stabilization problem for nonholonomic mobile robots is the use of time-varying state feedback, i.e. control laws that depend explicitly, not only on the state, but also on time, usually in a periodic way. Samson [13] introduced them in the context of the unicycle's point stabilization and raised the issue of the rate of convergence to the desired equilibrium.

In this section, we apply techniques of time-varying state feedback, recently developed by Morin and Samson [8], in a visual servoing framework [14].

The problem that we consider is to stabilize the mobile platform to the desired configuration which, without loss of generality, will be chosen to be zero, i.e.  $X^* = (x^*, y^*, \theta^*, \psi_1^*) = 0$ . The corresponding visual data  $Y_v^* = (Y_l^*, Y_m^*, Y_r^*)$  can be directly measured by putting the system in the desired configuration or can be easily specified, provided  $d$  is also known, along with the target geometry  $a$  and  $b$  (see figure 1).

An exponentially stabilizing control is considered for the mobile platform, while a control that keeps the targets foveated is considered for the camera.

**Mobile platform control synthesis :** In order to facilitate the synthesis of the controller, we apply a locally diffeomorphic transformation of the states and inputs

$$(x_1, x_2, x_3)^\top \stackrel{\text{def}}{=} (x, y, \tan \theta)^\top, \quad u_1 = \cos \theta v, \quad u_2 = \frac{1}{\cos^2 \theta} \omega, \quad (21)$$

which brings the unicycle kinematics (eq. 8) in the so-called *chained form* [11], [8]:

$$\dot{x}_1 = u_1, \quad \dot{x}_2 = x_3 u_1, \quad \dot{x}_3 = u_2. \quad (22)$$

The mobile platform control, that can be used if the state is known or reconstructed, is given by:

$$\begin{aligned} v(t, X) &= \frac{1}{\cos \theta} u_1(t, \Psi(X)), \\ \omega(t, X) &= \cos^2 \theta u_2(t, \Psi(X)), \end{aligned} \quad (23)$$

where  $u_1$  and  $u_2$  are the time-varying state-feedback controls, developed by Morin and Samson [8] for the 3-dimensional 2-input chained-form system. These controls, given in terms of the chained-form coordinates of equation 21, are :

$$\begin{aligned} u_1(t, x_1, x_2, x_3) &= k_1 [\rho_3(x_2, x_3) + \alpha(-x_1 \sin wt + |x_1 \sin wt|)] \sin wt, \\ u_2(t, x_1, x_2, x_3) &= -\frac{k_3}{\rho_3(x_2, x_3)} \left[ |u_1| x_3 + k_2 u_1 \frac{x_2}{\rho_2(x_2)} \right], \end{aligned} \quad (24)$$

where  $\rho_2(x_2) \stackrel{\text{def}}{=} |x_2|^{\frac{1}{3}}$ ,  $\rho_3(x_2, x_3) \stackrel{\text{def}}{=} (|x_2|^2 + |x_3|^3)^{\frac{1}{6}}$ ,  $w$  is the frequency of the time-varying controls and  $\alpha, k_1, k_2, k_3$  are positive gains. The exponential convergence to zero of the closed-loop system can be established using the homogeneous norm  $\rho(x_1, x_2, x_3) \stackrel{\text{def}}{=} (|x_1|^6 + |x_2|^2 + |x_3|^3)^{\frac{1}{6}}$ . The control  $\mathcal{U}$  for the mobile platform is then

$$\mathcal{U}(t, X) = (v(t, X), \omega(t, X))^\top. \quad (25)$$

Such a control requires an estimate  $\hat{X}$  of the current state  $X$ . This estimate can be provided by state reconstruction from the visual data [14]. However, since we are interested in positioning the mobile robot to the desired configuration  $X^* = 0$ , while starting relatively close to it, we could attempt to do so without reconstructing its state explicitly. Since  $Y = \Phi(X)$ , the state  $X$  can be approximated, near the configuration  $X^* = 0$ , up to first order by

$$\hat{X}(Y) = \left[ \frac{\partial \Phi}{\partial X}(X^*) \right]^{-1} (Y - Y^*), \quad (26)$$

where  $\frac{\partial \Phi}{\partial X} = B_2(X)B_1(X)$  with  $B_1$  and  $B_2$  as specified in 12 and 13 by setting  $n = 1$ . The proposed control law for the mobile platform can thus be expressed as a function of only the sensory data

$$\mathcal{U} = \mathcal{U}(t, Y). \quad (27)$$

**Arm control synthesis :** In order to implement a vision-based state-feedback control law for the mobile platform, we have to track the target during the motion of the platform. The arm control  $\omega_{\psi_1}$  is chosen to keep the targets foveated by regulating the angular deviation of the line-of-sight of the camera from the targets to zero, while the mobile robot moves. It is specified so that  $Y_m$  is made to decrease exponentially to  $Y_m^*$ , by regulating the task function  $e(X) \stackrel{\text{def}}{=} Y_m - Y_m^*$  to zero and by making the closed-loop system for  $e$  behave like  $\dot{e} = -\lambda e$ , for a positive gain  $\lambda$ . This gives

$$\omega_{\psi_1}(t, X, Y) = -\frac{\lambda}{\mathcal{J}_{2,3}}(Y_m - Y_m^*) - \left( \frac{\mathcal{J}_{2,1}}{\mathcal{J}_{2,3}} v + \frac{\mathcal{J}_{2,2}}{\mathcal{J}_{2,3}} \omega \right), \quad (28)$$

where  $\mathcal{J}_{2,i}$  is the  $(2, i)$ -entry of the matrix  $\mathcal{J}(X) \stackrel{\text{def}}{=} B_2(X) B_1(X) B_3(X)$ . In particular,  $\mathcal{J}_{2,3} = -f - \left( \frac{Y_m^2}{f} + \frac{l_2 f}{x_m^2} \right)$ . The first term of equation 28 makes the arm track the targets, while the term in parenthesis pre-compensates for the motion of the mobile robot. A useful simplification of this law can be obtained by ignoring this pre-compensation term.

**Experimental Results :** This control law has been validated by simulations and real experiments. Our test-bed is a unicycle-type mobile robot carrying a 6 d.o.f. manipulator arm with a CCD camera ([9],[15]).

In the experimental results presented below, we use the control law 27 with the unicycle controls 23, the arm control 28 and the state approximation 26 by sensory data. The following parameters corresponding to the models developed above are used:  $l_1 = 0.51 \text{ m}$ ,  $l_2 = 0.11 \text{ m}$ ,  $d = 2.95 \text{ m}$ ,  $f = 1 \text{ m}$ . The following gains are used for the above control laws:  $w = 0.1$ ,  $k_1 = 0.25$ ,  $k_2 = 2$ ,  $k_3 = 100$ ,  $\alpha = 10$ ,  $\lambda = 12$ . The controls 24 are normalized to avoid actuator saturation and wheel sliding; this does not affect the exponential stabilization of the system, only its rate.

Initial experiments used the raw visual data to calculate the state and the controls. Implementation of such a scheme leads to significant small oscillations and jerks during the motion of the system. To fix this problem, subsequent experiments used Kalman filtering of each of the state variables  $(x, y, \theta)$ . This makes the corresponding trajectories smoother and helps in compensating for the vision-induced delays. No filtering was used on the visual data. The resulting  $(x, y)$ -trajectory as well as the corresponding controls  $v$ ,  $\omega$  are plotted in figure 3. The dotted line represents data obtained by odometry, while the solid one represents data obtained by vision. Each period of the time-varying controls corresponds to 1570 samples (data on the state of the system are recorded every 40 msec).

### 3.3 Simultaneous Mobile Base and Camera Pose Stabilization:

The approaches in sections 3.1 and 3.2 can be seen as complementary. The first one can be used to stabilize the camera to a desired position and orientation

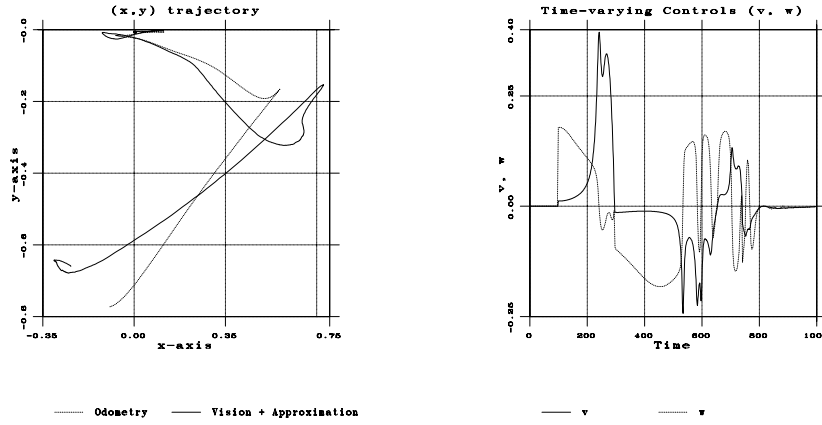


Figure 3: Mobile robot  $(x, y)$ -trajectory and controls  $v, \omega$

with respect to a target, but the final pose of the mobile basis is not controlled. The second one can stabilize the mobile basis to a desired pose with respect to a target and track this target with the camera while the robot moves, but it cannot independently stabilize the camera to a desired position and orientation. When additional d.o.f.s are available in the arm, they can be used to accomplish both goals simultaneously.

In this section we consider a mobile robot with a 3-d.o.f. arm as in fig. 1. Our goal is to simultaneously stabilize the mobile basis to a desired pose taken as  $\mathcal{X}^* = 0$  and the camera to a desired pose for which the corresponding visual data are  $Y_v^* \stackrel{\text{def}}{=} (Y_l^*, Y_m^*, Y_r^*)^\top$ .

The system state is  $X = (x, y, \theta, \psi_1, \psi_2, \psi_3)^\top$ , the measurement data are  $Y = (Y_l, Y_m, Y_r, \psi_1, \psi_2, \psi_3)^\top$  and the controls are  $\mathcal{U} = (v, \omega, \omega_{\psi_1}, \omega_{\psi_2}, \omega_{\psi_3})^\top$ .

The control components  $v$  and  $\omega$ , in charge of stabilizing the mobile platform can be determined as in section 3.2. The only difference is the state estimation, which is done by using matrices  $B_1$  and  $B_2$  that correspond to the present setup ( $n = 3$ ).

As in section 3.1, the camera pose stabilization is cast as the problem of regulating to zero the task function output  $e(X) \stackrel{\text{def}}{=} Y_v - Y_v^*$  with  $\dim e = 3$ . From 11 and the system kinematics, we get :

$$\dot{e} = \dot{Y}_v = B_{2,1}(X) (B_{1,1}(X) B_{1,2}(X)) B_3(X) \mathcal{U}. \quad (29)$$

where the matrices  $B_{1,1}$ ,  $B_{1,2}$ ,  $B_3$  are given in 6, 7 and 15, for  $n = 3$ . From 29, and since we want the equation  $\dot{e} = -\lambda e$ , to be satisfied for the controlled system, we get

$$B_{2,1}(X) B_{1,1}(X) B_{3,1}(X) \begin{pmatrix} v \\ \omega \end{pmatrix} + B_{2,1}(X) B_{1,2}(X) \begin{pmatrix} \omega_{\psi_1} \\ \omega_{\psi_2} \\ \omega_{\psi_3} \end{pmatrix} = -\lambda e. \quad (30)$$

Finally, solving for the arm controls  $\omega_{\psi_1}$ ,  $\omega_{\psi_2}$ ,  $\omega_{\psi_3}$  we get, away from singular configurations where  $B_{1,2}(X)$  and  $B_{2,1}(X)$  are not invertible,

$$\begin{pmatrix} \omega_{\psi_1} \\ \omega_{\psi_2} \\ \omega_{\psi_3} \end{pmatrix} = -\lambda B_{1,2}^{-1}(X)B_{2,1}^{-1}(X)(Y_v - Y_v^*) - B_{1,2}^{-1}(X)B_{1,1}(X)B_{3,1}(X) \begin{pmatrix} v \\ \omega \end{pmatrix}. \quad (31)$$

As previously, the first term of the above equation makes the arm track the targets, while the second term pre-compensates for the motion of the mobile basis. Notice that  $\det B_{1,2} = -l_1 l_2 \sin \psi_2$ , therefore configurations where it is zero are singular and should be avoided.

The validity of this control law has been tested in simulation. The  $(x, y)$ -trajectory of the mobile robot is very similar to the one in fig.3 and is not shown here.

## 4 Conclusion

We presented several approaches to the application of visual servoing techniques to hybrid holonomic/nonholonomic mechanical systems. How appropriate each of these approaches is, depends on the task to be performed and on the mechanical structure of the robot. The first approach, based on output linearization, proved to be robust with respect to modeling errors and measurement noise in both simulations and experiments. For tasks which only involve positioning the camera with respect to the robot's environment (e.g. target tracking, wall following, etc.), this first scheme applies. However, it does not apply anymore when the task explicitly requires stabilizing the nonholonomic platform to a desired pose, like, for example, in a parking maneuver. The second approach involving time-varying feedback techniques is, in this case, better adapted. The use of redundant systems allowing simultaneous stabilization of the camera and the nonholonomic platform brings up some exciting research issues in a large field of applications, like those where the robot has to navigate in highly constrained environments (e.g. nuclear plants or mine fields). The results presented here are however preliminary and their experimental evaluation is currently in progress using the test-bed described above. In particular, several theoretical and experimental issues need to be addressed concerning the robustness of such control schemes.

## References

- [1] R.W. Brockett, "Asymptotic Stability and Feedback Stabilization", in *Differential Geometric Control Theory*, Eds. R.W. Brockett, R.S. Millman and H.J. Sussmann, Birkhauser, Boston, 1983.
- [2] J.P. Laumond and al., "Robot Motion Planning and Control", Ed. J.P. Laumond, Lecture Notes in Control and Information Sciences, 229, Springer Verlag, 1997.
- [3] F. Chaumette, *La relation vision-commande: théorie et applications à des tâches robotiques*, Ph.D. Thesis, University of Rennes I, France, July 1990.

- [4] B. Espiau, F. Chaumette and P. Rives, "A New Approach to Visual Servoing in Robotics", *IEEE Trans. on Robotics and Automation* **8**, 313-326, 1992.
- [5] G.D. Hager and S. Hutchinson, Eds., "Vision-based Control of Robotic Manipulators", Special section of *IEEE Trans. Robotics and Automation* **12**, 649-774, 1996.
- [6] K. Hashimoto, Ed., *Visual Servoing*, World Scientific, 1993.
- [7] B.K.P. Horn, *Robot Vision*, Mc Graw-Hill, 1986.
- [8] P. Morin and C. Samson, "Application of Backstepping Techniques to the Time-Varying Exponential Stabilization of Chained Form Systems", INRIA Research Report No. 2792, Sophia-Antipolis, 1996
- [9] R. Pissard-Gibollet and P. Rives, "Applying Visual Servoing Techniques to Control a Mobile Hand-Eye System", *IEEE Intl. Conf. on Robotics and Automation*, 1995.
- [10] C. Samson, M. Le Borgne and B. Espiau, *Robot Control: The Task Function Approach*, Oxford University Press, 1991.
- [11] J.-B. Pomet and C. Samson, "Time-Varying Exponential Stabilization of Nonholonomic Systems in Power Form", INRIA Research Report No. 2126, Sophia-Antipolis, 1993.
- [12] P. Rives, R. Pissard-Gibollet and L. Pelletier, "Sensor-based Tasks: From the Specification to the Control Aspects", The 6th Intl. Symposium on Robotics and Manufacturing, Montpellier, France, May 28-30, 1996.
- [13] C. Samson, "Velocity and Torque Feedback Control of a Nonholonomic Cart", in *Advanced Robot Control*, Ed. C. Canudas de Wit, Lecture Notes in Control and Information Sciences, No. 162, Springer-Verlag, 1990.
- [14] D.P. Tsakiris, C. Samson and P. Rives, "Vision-based Time-varying Mobile Robot Control", Final European Robotics Network (ERNET) Workshop, Darmstadt, Germany, September 9-10, 1996. Published in *Advances in Robotics: The ERNET Perspective*, Eds. C. Bonivento, C. Melchiorri and H. Tolle, pp. 163-172, World Scientific Publishing Co., 1996.
- [15] D.P. Tsakiris, K. Kapellos, C. Samson, P. Rives and J.-J. Borrelly, "Experiments in Real-time Vision-based Point Stabilization of a Nonholonomic Mobile Manipulator", Preprints of the Fifth International Symposium on Experimental Robotics (ISER'97), pp. 463-474, Barcelona, Spain, June 15-18, 1997.
- [16] D.P. Tsakiris, P. Rives and C. Samson, "Applying Visual Servoing Techniques to Control Nonholonomic Mobile Robots", Workshop on "New Trends in Image-based Robot Servoing", International Conference on Intelligent Robots and Systems (*IROS'97*), pp. 21-32, Grenoble, France, September 8-12, 1997.